

PHYSICAL REVIEW B

CONDENSED MATTER

THIRD SERIES, VOLUME 51, NUMBER 14

1 APRIL 1995-II

Fractal structure of porous solids characterized by adsorption

S. J. Sze and T. Y. Lee*

Department of Chemical Engineering, National Tsing Hua University, Hsinchu, Taiwan 30043, Republic of China

(Received 23 May 1994; revised manuscript received 3 October 1994)

The fractal dimensions of porous solids, zeolites *A*, *X*, and Dowex MSC-1 were determined by physical adsorption and the values were 2.57, 2.37, and 2.92, respectively. In fact, it is counting the coverages of the adsorbate on the adsorbent. The solids can be visualized and simulated by a reducing similarity transformation. The resulting difference and significance of using the volume and area of the adsorbate to obtain the fractal dimensions are discussed.

INTRODUCTION

Fractal geometry has been developed and progressed rapidly in recent years (Mandelbrot,¹ Falconer,² Ross,³ and Schroeder⁴). It has been employed in the areas of biology (Peitgen and Richter⁵), climatology (Lorenz⁶), and engineering (Hibbert and Melrose⁷) to simulate the irregular shapes and chaotic movements. In general, fractals have two key elements: one is self-similarity and the other is fractal dimension. The self-similarity has a reducing or enlarging factor called *s* and the universal relationship between *s*, D_f (fractal dimension), and *N* (the number of fractal units) is $N = 1/s^{D_f}$. While D_f is normally not an integer, hence it is called fractal dimension in contrast to the conventional concept of geometry. Louis and Pereira⁸ suggested the application of the concept of the Menger sponge to the porous catalysts which might be characterized as the structure effects of the catalysts. Pfeifer and Avnir,⁹ Avnir,¹⁰ Avnir, Farin, and Pfeifer¹¹ in a series of papers demonstrated the application of adsorption isotherms to measure the fractal dimensions by consideration of the average area projection of the adsorbate on the available sites of the adsorbent. Radoev and Tenchov¹² discussed the fractal affect on the adsorption rate of porous solids. Sheituch and Brandon¹³ related the diffusion and reaction to the Thiele modulus of the catalysts.

In this study, the fractal dimensions of porous solids of zeolite 5A, zeolite X, and polymer Dowex MSC-1 are determined by the adsorption of different sizes of adsorbates. It is analogous to the classical example of using different length scale to measure the coastline of Britain. More properly the Hausdorff's dimension is adopted for box-counting area or volume. In fact, it is counting the coverages of the adsorbate on the adsorbent in this study. The resulting difference and significance of using the volume and area of the adsorbate are discussed.

THEORETICAL BACKGROUND

Mandelbrot¹ defined the fractal dimension as

$$D_f = \lim_{s \rightarrow 0} \frac{\log_{10} N}{\log_{10}(1/s)}, \quad (1)$$

where *s* is the measuring unit, *N* is the number of objects that can be measured by *s*, and D_f is the fractal dimension. For the *hD* space where *h* can be integers or fractional numbers, in case of *h* = 1, 2, or 3, we have

$$N(r) = Cr^{-D} \quad (2)$$

for

$$h = 1, \quad C = (\frac{1}{2})L,$$

$$h = 2, \quad C = \pi^{-1}A,$$

$$h = 3, \quad C = (\frac{3}{4})\pi^{-1}V.$$

This implies that length *r*, circle πr^2 , and sphere $(\frac{4}{3})\pi r^3$ are the measuring units. The measuring unit *s* in Eq. (1) should have a tendency to zero in order to eliminate the effect of geometric shapes on the fractal dimension. But, in practice, the measurement units should be varied in volume occupancy for fractal dimension of $2 \leq D_f \leq 3$, in area coverage for fractal dimension of $1 \leq D_f \leq 2$ and in line interval for $D_f \leq 1$ in order to obtain the realistic fractal dimensions. In this study, cross-section area coverage and volume occupancy adsorption isotherms of different size adsorbates are collected from literature to investigate the fractal structure of the porous solids and address their significance.

Following the same rationale, Eq. (2) can be transformed into

$$n(\sigma) = \mu\sigma^{-D_2+1}, \quad (3)$$

where σ is the molar cross-section area of adsorbed mole-

cules (McClellan and Harnsberger¹⁴), μ is the constant, n is the number of moles adsorbed and

$$n(v) = \eta v^{-D_3 + 1}, \quad (4)$$

where η is the constant and v is the molar volume of adsorbate.

Equations (3) and (4) are used for area coverage and volume occupancy isotherms, respectively. In case no experimental molar density or volume data are available, the corresponding state theory (Reid, Pravsnitz, and Sherwood¹⁵) is employed to estimate the molar volume used in Eq. (4). The fractal dimension D_i is based on area $i=2$ and on volume $i=3$, respectively, which is consistent with Pfeifer and Avnir.⁹ It is worth noting that Eq. (4), the fractal power of $-D_3 + 1$, certainly deserves further comment. Conceptually, the number of sorption sites can be visualized as measurement or coverage by a cube of length 1 (or sphere of radius r) of the sorbate molecules. If the sorbate molecules are not as regular as a cube or sphere, but rectangular ($1 \times h \times w$), then this extra irregular shape of $(1 \times h \times w - 1^3) = \text{fraction or multiple of } (1 \times h \times w) = k(1^3)$ has to be taken care of, that is, $\log_{10} N = \log_{10}(1^3)^{-D_3} + \log_{10} k(1^3)$. This first term is considered to be the effect of fractal power of regular shape whereas the second term is the correction of fractal power of irregular shape.

RESULTS AND DISCUSSION

Zeolite is aluminosilicate crystals and has a very rigid and uniform pore structure. Its structure has been studied extensively and identified (Breck¹⁶). In comparison, Dowex MSC-1 is an amorphous polymeric adsorbent. Its pore structure is random and irregular. Consequently, zeolite 5A (the Ca form of zeolite A), zeolite X, and Dowex MSC-1 were selected to represent a wide variety of porous solids in this study. From literature, the sorption capacities of different sizes of adsorbate on zeolite 5A,¹⁷⁻²⁹ zeolite X,³⁰⁻³⁷ and Dowex MSC-1 (Ref. 38) were obtained. A log-log plot of sorption capacity vs size of sorbate was prepared next. A regression line through the points was obtained from which the slope (after change sign) plus 1 was the fractal dimension of the solid characterized by adsorption as indicated by Eqs. (3) and (4). Employing the concept of the Menger sponge to represent the porous solid, we can construct and achieve a three-dimensional view of the porous solid generated by a deterministic process of repeatedly taking out a certain size of regular holes or slabs from the solid until it ended up with the same fractal dimension as the zeolites or Dowex MSC-1. The porous objects achieved by this reducing similarity process were served as the visualized solids.

Figures 1(a) and 1(b) are the capacity vs molar volume and capacity vs molar cross-section area plots on zeolite 5A, respectively. The slope (after change sign) plus 1 is the fractal dimension. Similarly, the plots for zeolite X and Dowex MSC-1 are shown in Figs. 2(a), 2(b), and 3(a), 3(b), respectively. All the fractal dimensions obtained are listed in Table I. It should be noted that the regression results are excellent with correlation coefficients ranging from 90 to 99%. The fractal dimensions obtained from

adsorbate volume plots are also more realistic and ranged from 2.37 to 2.92 falling in the fractals of porous solids with $2 \leq D_f \leq 3$, whereas the fractal dimensions derived from adsorbate cross-section area plots ranged from 2.69 to 3.29, and the 3.29 fractal suggested that it may be created from a four-dimensional solid and hence not realistic to represent a porous polymer. The reason sorbate volume as the measuring unit is more realistic than the sorbate cross-section area may be speculated in that the void in porous solids is three dimensional in nature, con-

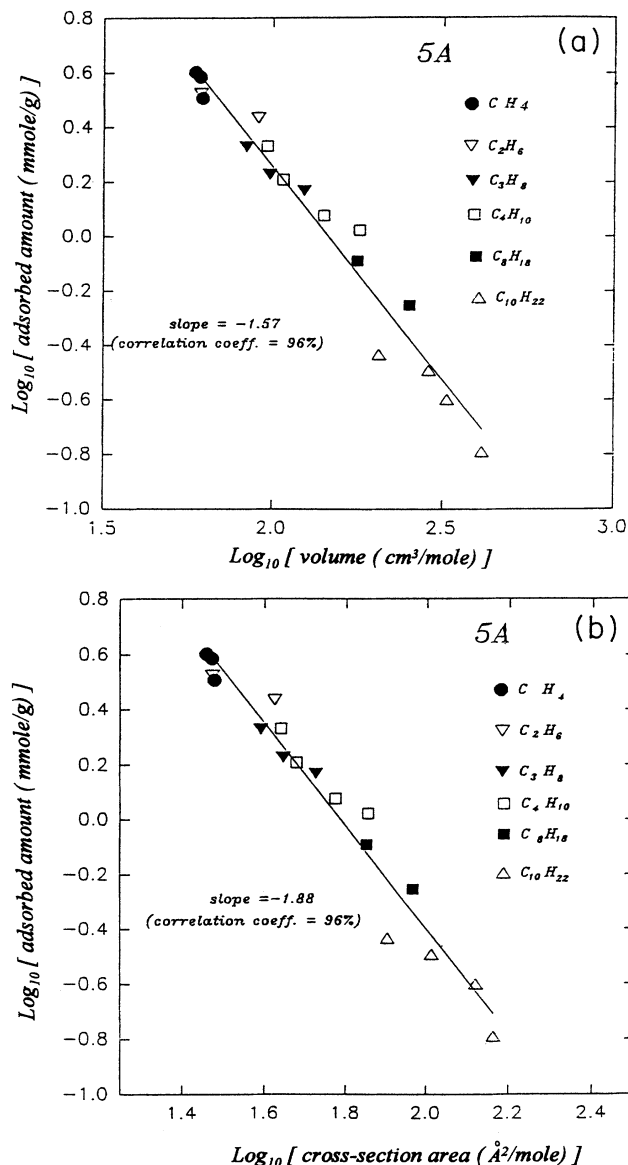


FIG. 1. (a) Adsorption capacity vs adsorbate molar volume. Data source: Danner and Wenzel (Ref. 17), Derrah *et al.* (Ref. 18), Haber *et al.* (Ref. 19), Kual (Ref. 20), Lederman and Williams (Ref. 21), Loughlin and Ruthven (Ref. 22), McClellan and Harnsberger (Ref. 14), Miller (Ref. 23), Reid *et al.* (Ref. 15), Ruthven and Loughlin (Ref. 24), Ruthven (Ref. 25), Sorial *et al.* (Ref. 26), Valitis *et al.* (Ref. 27), Verelst and Baron (Ref. 28), and Zuech *et al.* (Ref. 29). (b) Adsorption capacity vs adsorbate cross-section area. Data source: the same as data source of (a).

sequently, it is more reasonable to match the volume by volume. Furthermore, the cross-section area employed in this study is a projection of a sphere assumed for all the sorbates (McClellan and Harnsberger¹⁴), even though some sorbates are obviously cylindrical or long chained hydrocarbons. The two-dimensional projections may depend on the orientation of the sorbate inside the pore and this information cannot be correctly obtained at the present time.

The visualized solids of zeolite 5A, zeolite X, and

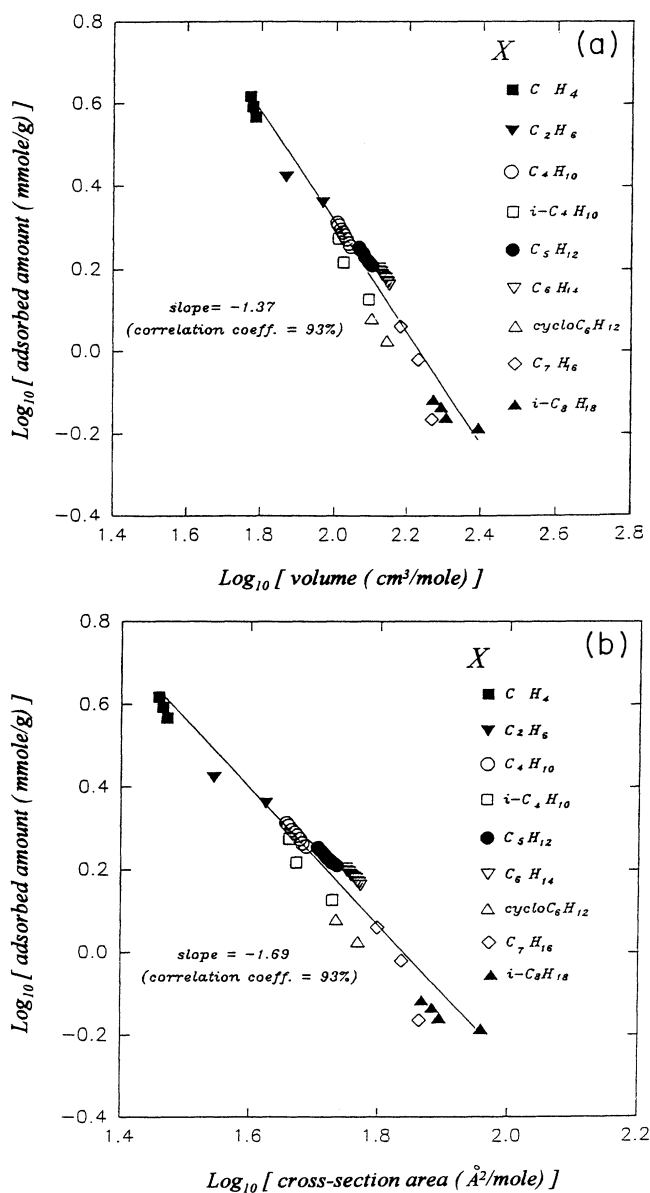


FIG. 2. (a) Adsorption capacity vs adsorbate molar volume. Data source: Barrer *et al.* (Ref. 30), Danner and Choi (Ref. 31), Danner *et al.* (Ref. 32), Hyun and Danner (Ref. 33), McClellan and Harnsberger (Ref. 14), Reid *et al.* (Ref. 15), Ruthven (Ref. 34), Ruthven and Francis (Ref. 35), Wukasugi *et al.* (Ref. 36), and Youngquit *et al.* (Ref. 37). (b) Adsorption capacity vs adsorbate cross-section area. Data source: the same as data source of (a).

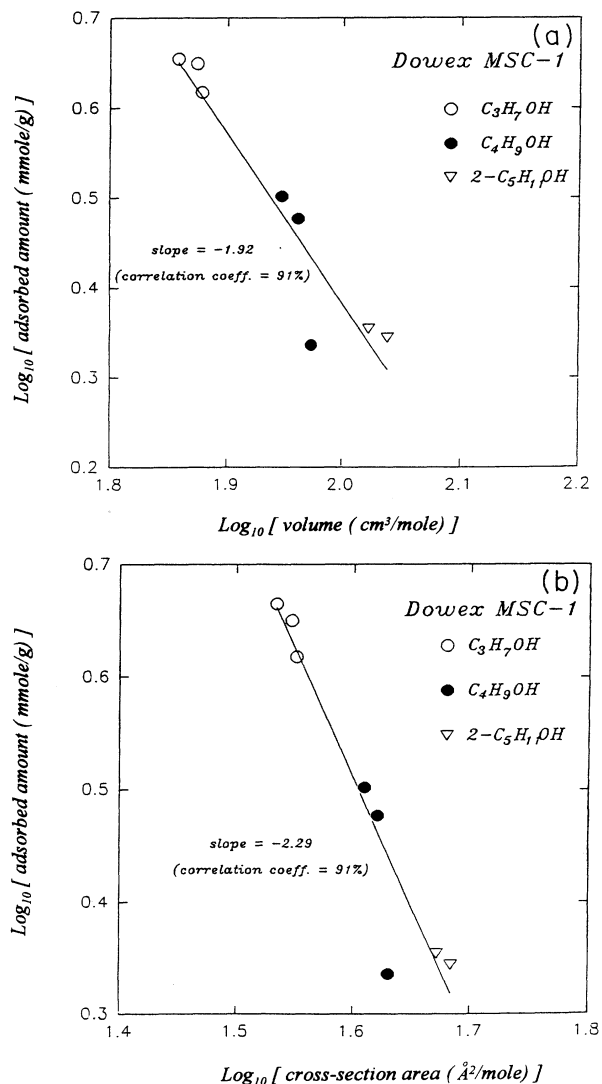


FIG. 3. (a) Adsorption capacity vs adsorbate molar volume. Data source: Chien (Ref. 38), McClellan and Harnsberger (Ref. 14), and Reid *et al.* (Ref. 15). (b) Adsorption capacity vs adsorbate cross-section area. Data source: the same as data source of (a).

Dowex MSC-1 are drawn in Figs. 4, 5, and 6, respectively. The construction of these solids was done through trial and error but Figs. 4 and 5 seem to be reasonable representations of zeolite 5A and zeolite X structure. Figures 4 and 5 are constructed by taking out $\frac{1}{5}$ and $\frac{1}{4}$ units in each of the X, Y, and Z directions, respectively. In the first step $m = 1$ both of the solids are left with eight sodalites as shown in Figs. 7 and 8. Differences are the lack of eight little connectors of either rectangular (for zeolite

TABLE I. The fractal dimensions of porous solids characterized by surface area and volume adsorption.

	Volume	Surface area
Zeolite 5A	2.57	2.88
Zeolite X	2.37	2.69
Dowex MSC-1	2.92	3.29

5A) or hexagonal prisms (for zeolite X) to the sodalites shown in the figures. Subsequently, repeating the same operation, we can create the solids with the same fractal dimension as characterized by the adsorption experiment. For instance, in the first step, $m = 1$, the total number of $\frac{1}{5}$ cubes are 125; 61 are taken out and 64 cubes are left. For j th step, $m = j$, $61 \times (64)^{j-1}$ number of $(\frac{1}{5})^j$ cubes are taken out and left are 64^j smaller cubes. Hence by Eq. (1) $D_f = \log_{10} 64 / \log_{10} 5 = 2.58$. Similarly, the fractal dimensions of 2.37 for zeolite X and 2.92 for Dowex MSC-1 are obtained. Although the visual picture of Dowex MSC-1 in Fig. 6 was constructed by the deterministic similarity transformation, the realistic random pore distribution can be represented nicely by the repeating regular pattern. It should be mentioned that the visualized porous solid did not have to be exactly like the real solid in all layers of structure, but it has to represent the sorption and possibly the transport properties as well as the fractal dimension of the real porous solid effectively.

It is interesting to see how the chaos game can create the porous structure of Fig. 6. For easy explanation, let us consider a flat view of two-dimensional Fig. 6. The four points of the square can be denoted by A, B, C, and D. Let us use a fair die to represent either point A, B, C, or D, respectively. Then take any point x_0 inside the square and throw the die. If a face shows up representing point C, then connect the x_0 C line. Denote the one-fifth distance of the line segment as point x_1 . Repeating this procedure n times, n could be 5000 or 50 000, n points will be obtained, then the upper parts of Fig. 6 will emerge gradu-

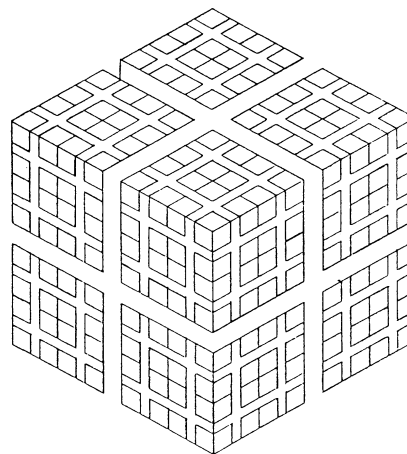
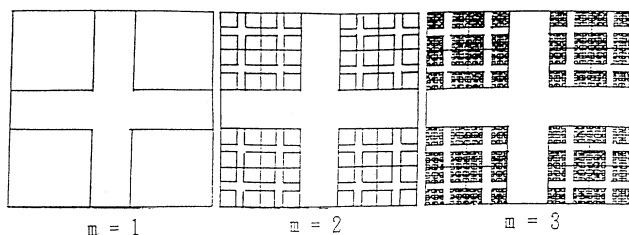


FIG. 5. Visualized X zeolite.

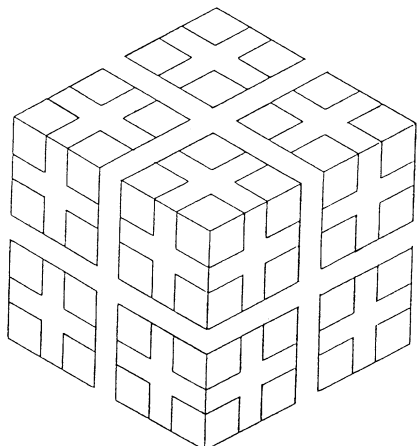
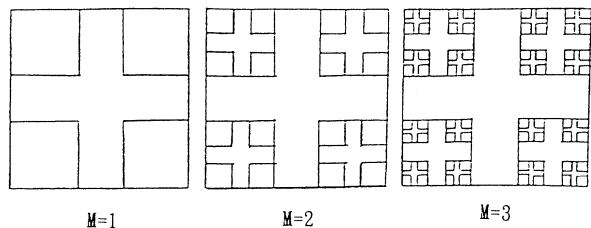


FIG. 4. Visualized 5A zeolite.

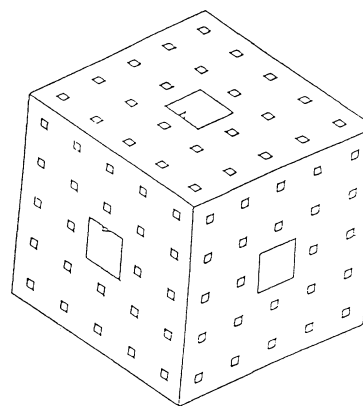
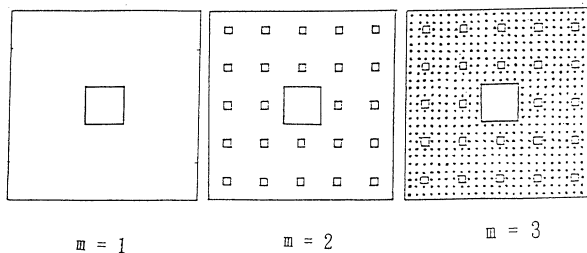


FIG. 6. Visualized Dowex MSC-1.

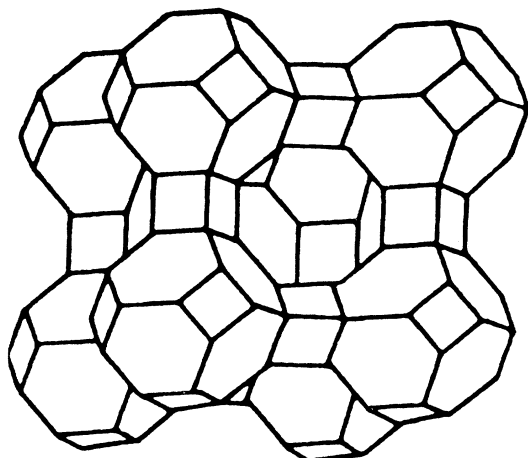


FIG. 7. A-zeolite structure.

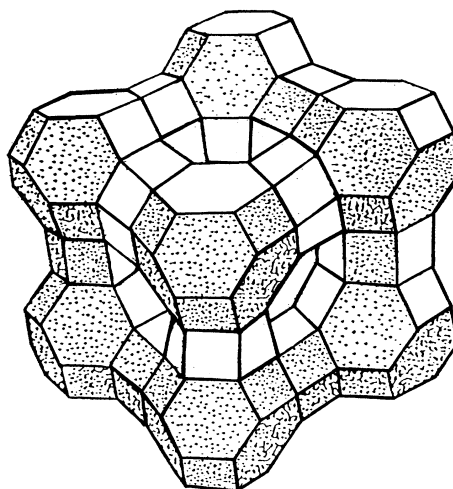


FIG. 8. X-zeolite structure.

ally. Next, let us explain the formation of the porous structure of Fig. 4. Again, a two-dimensional view is used for easy explanation. Instead of building a Cantor quinary set in a line segment, we can build a Cantor quinary set in a square in the same way (Mandelbrot¹). If we use the coordinate system (x,y) and take $(0,0)$, $(1,0)$, $(0,1)$, and $(1,1)$ as the vertices of the square. The arbitrary point in the square of the Cantor quinary set will correspond to coordinate (x,y) . Both x and y belong to the Cantor quinary set, that is x or y falls in one of the five equal segments of the unit x or y axis. If it is in the middle one-fifth segment then that whole section is taken out. Repeating this process in the remaining smaller squares, the results were shown in the upper parts of Fig. 4. If the squares were addressed in quinary systems of 2 digit, 4 digit, . . . , and $2n$ digit, even smaller squares, it could be

an interesting chaos game on a computer screen. In this fashion, Figs. 4, 5, and 6 were created by extension to three dimension.

CONCLUSIONS

The fractal structure of a porous solid can be characterized by adsorption of different sizes of volume adsorbates. The fractal solid can be constructed and visualized by reducing similarity transformation. The possible effects on the transport properties of the fractal solid may be investigated by the formation of mass and energy balance equations in which the fractal dimension was incorporated.

*To whom correspondence should be addressed.

¹B. B. Mandelbrot, *The Fractal Geometry of Nature* (Freeman, New York, 1983).

²K. Falconer, *J. Chem. Eng.* **49**, 1 (1992).

³B. Ross, *Fractal Calculus and its Applications* (Springer, Berlin, 1974).

⁴Mantred Schroeder, *Fractals, Chaos, Power Laws* (Freeman, New York, 1991).

⁵H.-O. Peitgen and P. H. Richter, *The Beauty of Fractals* (Springer, Berlin, 1986).

⁶E. N. Lorenz, *J. Atmos. Sci.* **20**, 130 (1963).

⁷D. B. Hibbert and J. R. Melrose, in *Fractals in the Natural Science*, edited by M. Fleischmann, D. J. Tildesley, and R. C. Ball (Princeton University Press, Princeton, 1990), p. 149.

⁸L. Louis and C. J. Pereira, *Chem. Eng. Sci.* **45**, 2027 (1990).

⁹Peter Pfeifer and David Avnir, *J. Chem. Phys.* **79**, 3558 (1983).

¹⁰David Avnir, *Chem. Ind.* **16**, 912 (1991).

¹¹David Avnir, Dina Farin, and Peter Pfeifer, *New J. Chem.* **16**, 439 (1992).

¹²B. P. Radoev and B. G. Tenchov, *J. Phys. A* **20**, L159 (1987).

¹³Moshe Sheituch and Shimon Brandon, *Chem. Eng. Sci.* **44**, 69 (1989).

¹⁴A. L. McClellan and H. F. Harnsberger, *J. Colloid Interface Sci.* **23**, 577 (1967).

¹⁵R. C. Reid, John M. Prausnitz, and T. K. Sherwood, *The Property of Gases and Liquid* (McGraw-Hill, New York, 1977).

¹⁶D. W. Breck, *Zeolite Molecular Sieve* (Wiley, New York, 1974).

¹⁷R. P. Danner and L. A. Wenzel, *AIChE J.* **15**, 515 (1969).

¹⁸R. I. Derrah, K. F. Loughlin, and D. M. Ruthven, *J. Chem. Soc. Faraday Trans.* **68**, 1947 (1972).

¹⁹J. Haber, J. Najbar, J. Pawelek, and J. Pawlikowska-Czubak, *J. Colloid Interface Sci.* **45**, 252 (1973).

²⁰Bal K. Kaul, *Ind. Eng. Chem. Res. Dev.* **26**, 928 (1987).

²¹P. B. Lederman and Brymer Williams, *AIChE J.* **10**, 30 (1964).

²²K. F. Loughlin and D. M. Ruthven, *J. Colloid Interface Sci.* **39**, 331 (1972).

²³G. W. Miller, *AIChE J.* **33**, 194 (1987).

²⁴D. M. Ruthven and K. F. Loughlin, *J. Chem. Soc. Faraday Trans.* **68**, 696 (1972).

²⁵D. M. Ruthven, *AIChE J.* **22**, 753 (1976).

²⁶G. A. Sorial, W. H. Granville, and W. O. Daly, *Chem. Eng. Sci.* **38**, 1517 (1983).

- ²⁷A. P. Valitis, D. M. Ruthven, and K. F. Loughlin, *J. Colloid Interface Sci.* **84**, 526 (1981).
- ²⁸Harry Verelst and V. Baron Gino, *J. Chem. Eng. Data* **30**, 66 (1985).
- ²⁹J. L. Zuech, Anthony L. Hines, and Sloan E. Dendy, *Ind. Eng. Chem. Prod. Res. Dev.* **22**, 172 (1983).
- ³⁰R. M. Barrer and J. W. Suthorland, *J. Am. Chem. Soc. London Ser. A* **237**, 439 (1956).
- ³¹R. P. Danner, M. P. Nicoletti, and Rasheeds Al-ameeri, *Chem. Eng. Sci.* **35**, 2129 (1980).
- ³²R. P. Danner and Edwin C. F. Choi, *Ind. Eng. Chem. Fundam.* **17**, 248 (1978).
- ³³Sang H. Hyun and R. P. Danner, *J. Chem. Eng. Data* **27**, 196 (1982).
- ³⁴D. M. Ruthven, *AIChE J.* **27**, 654 (1981).
- ³⁵D. M. Ruthven and Wong Francis, *Ind. Eng. Chem. Fundam.* **24**, 27 (1985).
- ³⁶Yuji Wakasugi, Sentaro Ozawa, and Yoshisada Ogino, *J. Colloid Interface Sci.* **79**, 3990 (1981).
- ³⁷G. R. Youngquit, L. James Allen, and Joseph Eisenberg, *Ind. Eng. Chem. Prod. Res. Dev.* **10**, 308 (1971).
- ³⁸Shih-Chen Chien and Ting-Yue Lee, *J. Chin. Inst. Eng.* **8**(1), 17 (1985).